



Nitrogen cycling and origin of ammonium during infiltration of treated wastewater for managed aquifer recharge

Matthew Silver^{a,b,*}, Kay Knöller^c, Johanna Schlägl^a, Christine Kübeck^b, Christoph Schüth^{a,b}

^a Technische Universität Darmstadt, Institute of Applied Geosciences, Schittspahnstraße 9, Darmstadt, 64287, Germany

^b IWW Water Centre, Moritzstraße 26, Mülheim an der Ruhr, 45476, Germany

^c UFZ Helmholtz Centre for Environmental Research, Department of Catchment Hydrology, Theodor-Lieser-Straße 4, 06120, Halle (Saale), Germany

ARTICLE INFO

Editorial handling by J. Mirecki

Keywords:

Wetting and drying cycles

Redox conditions

Ammonification

Nitrification

DNRA

Stable isotopes

ABSTRACT

As more regions in the world look to replenish depleted aquifers, treated wastewater (TWW) is increasingly infiltrated in managed aquifer recharge (MAR) schemes. While MAR is a promising emerging technology, it also has the potential to generate pollutants along the infiltration flow path. In this study, we infiltrated treated wastewater through an organic-rich soil in column experiments operated with wetting and drying cycles. Ammonium, which was present only in trace concentrations in the TWW, increased in concentration with depth and exceeded the EU Water Framework Directive limit of 0.5 mg/L for up to a year, depending on the sampling depth. Pore water samples collected at the end of drying periods showed very high nitrate concentrations, indicating nitrification of some of the ammonium. Oxidation reduction potential often exceeded 200 mV during drying periods, showing conditions for nitrification, but dropped below -100 mV during wetting periods, creating several possible pathways for ammonium production. Potential sources of ammonium are (1) dissolved organic nitrogen in the TWW, (2) nitrate in the TWW, and (3) organic nitrogen in the soil. $\delta^{15}\text{N}$ in ammonium in pore water samples (mean 4.7‰) was slightly higher than $\delta^{15}\text{N}$ in the soil (2.4‰), indicating that the soil was likely the major source but also that nitrate (mean 17.2‰) may have been the source of some of the ammonium. Fractionation of ^{15}N in nitrate as well as high concentrations of acetate (a labile organic carbon source) also indicate that dissimilatory nitrate reduction to ammonium may have formed some of the NH_4^+ .

1. Introduction

Managed aquifer recharge (MAR) is an emerging technology to address water scarcity by recharging depleted aquifers. Infiltration of treated wastewater (TWW) has been demonstrated to efficiently attenuate viruses present in the TWW (Powelson et al., 1993) and is also effective to varying extents at removing anthropogenic organic compounds such as pharmaceuticals present in the TWW (Maeng et al., 2011; Silver et al., 2018). While much has been studied about the fate of pathogens and pollutants present in TWW, there has been less focus on pollutants that can be generated along the infiltration flow path. In some MAR applications, nitrate persists in the recharged water (Bekele et al., 2011), while in others, nitrate has been attenuated by adding a reactive, organic-rich surface layer (Valhondo et al., 2015). While this technique is effective for nitrate and other compounds, it has the potential to generate ammonium. Ammonium has a much lower drinking water limit of 0.5 mg/L compared to nitrate (50 mg/L) (The Council of

the European Union, 1998) and both are relevant to the status of surface water and groundwater (The Council of the European Union, 2000). The present study considers the redox conditions when TWW is infiltrated through a soil with high organic matter content, and in particular, the effects on nitrogen compounds.

Infiltration in MAR applications is commonly conducted in wetting and drying cycles (Bouwer, 2002; Morugán-Coronado et al., 2011; Goren et al., 2014; Barry et al., 2017), which are effective at re-introducing oxygen to the subsurface at least at the macro scale (Dutta et al., 2015). Wastewater treatment effluents contain dissolved organic nitrogen (DON), often in concentrations of 1–2 mg/L (Parkin and McCarty, 1981; Czerwionka et al., 2012), as well as dissolved inorganic nitrogen (DIN). In MAR applications, both nitrified-denitrified (DIN is mostly nitrate) and conventional secondary (DIN is mostly ammonium) effluents have been infiltrated (Kopchynski et al., 1996). Infiltration of conventional secondary effluent can result in elimination of ammonium mass through a combination of retardation preventing fast transport,

* Corresponding author. Technische Universität Darmstadt, Institute of Applied Geosciences, Schittspahnstraße 9, Darmstadt, 64287, Germany.

E-mail addresses: silver@geo.tu-darmstadt.de (M. Silver), kay.knoeller@ufz.de (K. Knöller), johanna.schloegl@uni-tuebingen.de (J. Schlägl), c.kuebeck@iww-online.de (C. Kübeck), schueth@geo.tu-darmstadt.de (C. Schüth).

<https://doi.org/10.1016/j.apgeochem.2018.08.003>

Received 9 April 2018; Received in revised form 15 July 2018; Accepted 1 August 2018

Available online 02 August 2018

0883-2927/ © 2018 Elsevier Ltd. All rights reserved.

Table 1

Nitrogen transforming reactions based on acetate ($C_2H_3O_2^-$) as the organic carbon source. The nitrite ion (NO_2^-) is omitted for simplification.

Process name	Chemical reaction
Nitrification	$NH_4^+ + 2O_2 \rightarrow NO_3^- + 2H^+ + H_2O$
Denitrification	$4NO_3^- + 3C_2H_3O_2^- \rightarrow 2N_2 + 6HCO_3^- + 3H^+$
Dissimilatory nitrate reduction to ammonium (DNRA)	$NO_3^- + C_2H_3O_2^- + H^+ + H_2O \rightarrow NH_4^+ + 2HCO_3^-$

nitrification during drying periods, and denitrification (Table 1) and/or anaerobic ammonium oxidation (also known as ANAMMOX) during wetting periods (Miller et al., 2006; Goren et al., 2014; Hernández-Martínez et al., 2016). This combination of processes, however, has resulted in low (apparent) nitrogen elimination rates in several MAR field applications: around 20% at Alice Springs, Australia (Barry et al., 2017), or up to 42% in one instance (Miotlinski et al., 2010); 0–30% at Flushing Meadows, Arizona, USA, as well as rates close to 50% at Dan Region, Israel and Sweetwater, Arizona, USA (Miller et al., 2006); and temporally and spatially varying elimination as low as 30% at Harkins Slough, California, USA (Schmidt et al., 2012). Although small increases in ammonium concentrations during infiltration were observed at the Dan Region site by Goren et al. (2014), the possibility of ammonium production within MAR schemes has not been widely studied.

In a system with TWW infiltrated through a soil with organic matter, several sources of nitrogen are present: DON in the TWW, nitrate in the TWW, and organic nitrogen in the soil. Bekele et al. (2011) report nitrification from both ammonium and DON in a calcareous aquifer, but nitrate remained present as oxidizing conditions persisted. Based on the nitrogen mass balance, some DON had to have been ultimately converted to nitrate (Bekele et al., 2011), possibly with DON being mineralized to ammonium in an initial step. In a laboratory study infiltrating artificial wastewater, Essandoh et al. (2011) found that ammonium was produced from DON. Another possible source of ammonium is nitrate. Infiltration of nitrate in soils under reducing conditions often leads to denitrification, but the process dissimilatory nitrate reduction to ammonium (DNRA) can also occur (Buresh and Patrick, 1978). Recent research suggests that some microorganisms are able to do both nitrate reducing processes (Mania et al., 2014; Yoon et al., 2015), and that the environmental conditions rather than specific microbial species determine the end product (Kraft et al., 2014). Most researchers agree that higher C:N ratios make DNRA more likely, but the exact environmental controls are not known. Finally, the soil organic matter is a possible source for ammonium. Some soils contain a substantial fraction of mineralizable nitrogen (Stanford and Smith, 1972), which can be accessed by soil microbes to form ammonium (Hadas et al., 1992; Murphy et al., 2003). Positive but low $\delta^{15}N-NH_4^+$ values have indicated formation of ammonium in aquifers from mineralization of soil organic matter (Lingle et al., 2017; Caschetto et al., 2017).

To characterize and evaluate the production of ammonium in a MAR-like system, we performed soil column experiments, infiltrating TWW through a soil with substantial organic matter content. Two experiments were conducted: a long-term experiment (CI) lasting approximately 615 days, and a short-term experiment (CII) lasting 140 days to study ammonium-forming processes in more detail. In both experiments, soil pore water samples were collected from sampling ports along the length of the column. In the long-term experiment, samples were only measured for ions, but the total time of the experiment provides an overview of the leaching and transport of ammonium that can be expected and the time necessary for ammonium concentrations to fall below the EU drinking water standard. In the short-term experiment, samples were also measured for ions, including acetate (a form of labile organic carbon that could influence nitrate reduction), as well as for stable isotopes in nitrate and ammonium.

Since nitrate is a possible source of ammonium, isotopic data related to the fate of nitrate were also collected. Oxygen concentrations were measured to provide information related to nitrification and denitrification. With these data, the overall purpose of this work is to evaluate the source(s) and mode of origin of ammonium produced in a system simulating MAR.

2. Materials and methods

2.1. Soil and inflow water

The experimental soil was obtained from non-agricultural grassland approximately 12 km northeast of Athens, Greece, immediately west of the Dimosio Dasos Rapentosas wildlife refuge, at a possible future MAR site. Disturbed soil samples were collected over two days and packaged in plastic-coated aluminum bags. The soil is a loamy sand and contains $2.57\% \pm 0.01\%$ organic carbon and $0.221\% \pm 0.002\%$ nitrogen based on three subsets of milled soil analyzed with an Elementar CNS analyzer.

TWW was collected at least once per week, from a municipal wastewater treatment plant in Darmstadt, Germany, for experimental inflow water. The water was collected in a 15-L glass jug. In the TWW, nitrate averaged 1.96 mg of nitrogen per liter [mg(N)/L] and dissolved organic carbon averaged 7.3 mg/L (Table 2), while DON was measured in the range of 1.4–2.1 mg/L in three samples from the short-term experiment (see Appendix A, supplementary information (SI)). The analytical methods are described in section 2.4 (ions and DON) and the SI (dissolved organic carbon).

2.2. Column experiments and sampling

The experimental columns consisted of an acrylic glass pipe (length: 1 m, inner diameter: 0.19 m) connected to a lid and base plate, also made out of acrylic glass. Inflow water was stored in a 15-L glass jug, pumped out via polytetrafluoroethylene (PTFE) tubing, through a peristaltic pump using a short (~20 cm) section of Tygon® tubing, and to the column through another section of PTFE tubing and a stainless steel threaded connector. Flow was from the top of the column downward, in order to conduct infiltration with wetting and drying cycles in a similar manner to field conditions. The outflow was collected in a bucket, which was weighed empty and full to obtain the volume of water (assumed density 0.998 g/cm^3).

Cycles were typically three to four days of wetting and three to four days of drying. During the 16th wetting period in the short-term experiment, a tracer test was conducted lasting 15 days. The hydraulic loading was approximately 7 cm/d in the long-term experiment and 3.5 cm/d in the short-term experiment, due to differences in hydraulic conductivity, resulting in the exchange of 1–2 pore volumes during each wetting phase. The long-term experiment lasted for 615 days and the short-term experiment for 140.5 days. A schematic of the columns is shown in the SI, Figure S1.

Sampling at the end of wetting phases was conducted by first taking a sample from the uppermost port and then proceeding downward, in the direction of the water flow. In this way, samples were collected with

Table 2

Composition and variation of the inflow TWW. The summarized data reflect samples collected for the long-term experiment.

	Nitrate nitrogen mg(N)/L	Ammonium nitrogen mg(N)/L	Dissolved organic carbon mg(C)/L
min	1.07	0.02	2.7
mean	1.96	0.17	7.3
median	1.74	0.11	6.6
max	4.36	0.76	14
n	35	35	16

as little disruption as possible to the flow velocity at the time of sampling at each port. Samples were collected in polypropylene or high density polyethylene sample bottles. Measurement of pH was done using a WTW Multi 340i meter and pH electrode, immediately following sample collection.

In order to obtain samples of water present in the pore space at the end of the drying phases, a method called “first flush” sampling was developed. The premise of the first flush sampling is that residual pore water is carried on top of the rising water table during the filling of the column. While water was pumped into the column, samples were collected as soon as water began to flow out of each sampling port, starting with the lowest sampling port (75 cm) and working upwards as the water table rose. All ports were opened beforehand and samples were taken as soon as the first flush of water came out of the ports. The focus of first flush sampling was on changes in nitrogen species, which are sensitive to oxidation-reduction conditions. To evaluate the impact of mixing of pore water (the water targeted for sampling) with inflow water, the composition of the inflow water was also measured. Further, during one first flush sampling event, sodium bromide salt was added to the inflow water and the bromide ion used as a tracer for the portion of inflow water sampled. The background concentration of bromide in the soil columns is low (usually less than 1.5 mg/L). The bromide ion was measured in all samples using ion chromatography. The bromide concentration found in each sample then allowed estimation of how much inflow water was sampled and therefore how much of the sample contained pore water.

2.3. Oxygen and oxidation reduction potential

To monitor conditions related to nitrification and denitrification, oxygen concentrations were measured with an oxygen sensing system from Presens GmbH (Regensburg, Germany). Sensor spots (type PS3t, detection limit 0.001 mg/L) were fixed to the inside of the column walls at depths below the soil surface of 0, 2, 7, 12, 19.5, 27, 42, 57, and 72 cm on CI (concentration-depth profiles collected) and 15 cm on CII (time series collected). Oxygen concentrations were read using a fiber-optic cable connected to a Presens Fibox3 control unit.

In the short-term experiment, oxidation reduction potential (ORP) was measured using an in-situ probe (similar to the probe used by Vorenhout et al. (2004)) manufactured by Paleo Terra (Amsterdam, the Netherlands) and a QIS (Oosterhout, the Netherlands) QM710X reference electrode (3.0 Molar KCl saturated with AgCl). Measurement of ORP was done in order to have a continuous indication of the oxidation-reduction state of the soil, through all parts of the wetting and drying cycles. The in-situ probe consists of platinum sensors at five depths. The reference electrode was placed in the uppermost part of the soil, where it serves as a reference for any one of the five platinum tip sensors. The platinum sensors and reference electrode were connected to a Campbell Scientific CR800 data logger, which made voltage measurements for each platinum sensor. The voltage measurements were adjusted to values of a standard hydrogen electrode by adding 212 mV to each measurement.

2.4. Ions and total bound nitrogen

Water samples were measured for nitrate, bromide, and acetate with a Metrohm (Herisau, Switzerland) 882 Compact IC plus – Anion (carbonate eluent) and for ammonium with a Metrohm 882 Compact IC plus – Cation (dicarboxylic acid and nitric acid eluent). Samples were diluted prior to measurement, resulting in detection limits of approximately 0.025 mg/L for nitrate, 0.1 mg/L for acetate and 0.05 mg/L for ammonium. Acetate was measured along with inorganic anions (Krata et al., 2009) after calibrating with an acetate standard solution (Carl Roth, Germany).

The mass of ions passing each sampling location over the duration of the experiments is calculated from the ion concentrations and

measured flow volume. The calculations were performed using trapezoidal numerical integration of all available data points. The width of each trapezoid corresponded to the elapsed flow volume between the sampling events and the upper slope of each trapezoid connected the concentrations from consecutive sampling events. The areas of all trapezoids were summed to obtain total mass.

Selected samples of inflow water were measured for total bound nitrogen (tN_b) using the U.S Geological Survey method for alkaline persulfate digestion (Patton and Kryskalla, 2003), adapted for measurement of nitrate by ion chromatography as follows: 2 mL of each sample was combined with a solution of potassium persulfate in potassium hydroxide and then heated in a closed vessel for 1 h at 148 °C. Afterwards, the samples were allowed to cool to room temperature. Then, they were diluted 30 times and nitrate was measured by ion chromatography. The digestion reagent contained nitrogen, so triplicate reagent blanks were carried through the entire process to correct the results for reagent nitrogen. Standards of urea (organic nitrogen) were also carried through the process.

2.5. Isotopes

Samples were kept frozen prior to isotope analysis. Subsamples were used for measurement of isotopes in ammonium and nitrate.

Samples for $\delta^{15}N$ analysis of ammonium were prepared based on a modified Kjeldahl method that is suitable for sample volumes smaller than 50 mL. Pure sulfuric acid (0.05 N) was added to 50 mL aliquots of the water samples upon defrosting to preserve ammonium. After adjusting alkaline conditions by adding 32% NaOH solution and bromothymol blue for visual pH control, sample ammonium was transferred to a trapping flask containing 0.05N H_2SO_4 by distillation for 30 min. Any trapping liquid was evaporated in a sand bath at 80 °C. The solid residue was homogenized and weighed for combustion in an elemental analyzer (vario isotope cube, Elementar) connected to an isotope ratio mass spectrometer (IsoPrime100).

Measurement of stable isotopes of nitrate ($\delta^{15}N$ and $\delta^{18}O$) was conducted on 0.2 μm filtered (sterile cellulose acetate membranes) with 10 mL aliquots of the original defrosted samples. Stable isotope ratios were measured on a GasbenchII/delta V plus combination (Thermo) using the denitrifier method for simultaneous determination of $\delta^{15}N$ and $\delta^{18}O$ in the measuring gas N_2O , produced by controlled reduction of sample nitrate (Sigman et al., 2001; Casciotti et al., 2002; McIlvin and Casciotti, 2011).

Apparent enrichment factors (ϵ) of nitrate were calculated from results of the inflow and a sample collected from depth in the soil by solving

$$\delta = \delta_0 + \epsilon \ln(C/C_0) \quad (1)$$

for ϵ , where δ is the measured isotopic ratio at depth, δ_0 is the measured isotopic ratio in the inflow water, C is the nitrate concentration at depth, and C_0 is the nitrate concentration in the inflow water.

Samples of the inflow TWW were measured for tN_b concentration and isotopes. With results for tN_b and DIN, DON concentrations were calculated by difference:

$$C_{DON} = C_{tN_b} - C_{DIN} \quad (2)$$

$\delta^{15}N$ -DON is calculated by mass balance:

$$\delta^{15}N-DON = (\delta^{15}N-tN_b * C_{tN_b} - \delta^{15}N-NO_3 * C_{NO_3}) / C_{DON} \quad (3)$$

Samples were prepared for tN_b isotope measurements by first evaporating the water at 60 °C in a sand bath to a volume of 15–20 mL, which was then placed in a concentrator (Eppendorf Concentrator 5301) until only solid remained. As for isotope analysis of NH_4 , aliquots of the homogenized solid were then combusted in an elemental analyzer (vario isotope cube, Elementar) connected to an isotope ratio mass spectrometer (IsoPrime100). Some samples were measured after longer

storage time (frozen at 20 °C, ca. 5–12 months after collection) and more solid material appeared stuck to the walls of the HDPE sample bottles, resulting in lower solid yields. Results from these samples are discarded and only results from samples frozen for a short time (less than 9 weeks) before analysis are reported. For these samples, no precipitate or material stuck to the sample bottle was visible.

Samples for measurement of $\delta^{15}\text{N}$ in the original soil were milled to a grain size of < 100 μm . Approximately 30 mg of milled soil was combusted in an elemental analyzer (vario isotope cube, Elementar) connected to an isotope ratio mass spectrometer (IsoPrime100).

Nitrogen and oxygen isotope results are reported in delta notation ($\delta^{15}\text{N}$, $\delta^{18}\text{O}$) as part per thousand (‰) deviation relative to the standards AIR for nitrogen and VSMOW for oxygen (general equation (1)), where R is the ratio of the heavy to light isotopes (e.g. $^{15}\text{N}/^{14}\text{N}$; $^{18}\text{O}/^{16}\text{O}$).

$$\delta_x (\text{‰}) = [(R_{\text{sample}} - R_{\text{standard}}) / R_{\text{standard}}] \times 1000 \quad (4)$$

The standard deviation of the nitrogen isotope analysis of nitrate, ammonium and tN_b is $\pm 0.4\text{‰}$. Oxygen isotope analysis of nitrate is conducted with a precision of better than $\pm 1.6\text{‰}$. For calibration of nitrogen and oxygen isotope values of nitrate samples, the reference nitrates IAEA-N3 ($\delta^{15}\text{N}$: +4.7‰ AIR; $\delta^{18}\text{O}$: +25.6‰ VSMOW) USGS32 ($\delta^{15}\text{N}$: +180‰ AIR; $\delta^{18}\text{O}$: +25.7‰ VSMOW), USGS 34 ($\delta^{15}\text{N}$: -1.8‰ AIR; $\delta^{18}\text{O}$: -27.9‰ VSMOW), and USGS 35 ($\delta^{15}\text{N}$: +2.7‰ AIR; $\delta^{18}\text{O}$: +57.5‰ VSMOW) were used. Calibration of ammonium and tN_b isotope values was based on the standards USGS 25 ($\delta^{15}\text{N}$ = -30.4‰), USGS 26 ($\delta^{15}\text{N}$ = 53.70‰) and an internal standard NH4-0 ($\delta^{15}\text{N}$ = 0‰).

3. Results and discussion

Results of the long-term experiment are presented and discussed to characterize ammonium concentrations and some aspects of redox conditions during the wetting and drying cycles. Results of the short-term experiment are then presented, first establishing relevant redox conditions and then moving to ammonium concentrations and stable isotopes in nitrogen species.

3.1. Long-term experiment

3.1.1. Wetting periods

Oxygen was consumed in 2–8 h in the range of 2–12 cm depth after beginning the third wetting period (Figure S2) and it is presumed that depletion of oxygen occurred over a similar time period during other wetting periods. Ammonium concentrations rose in the beginning of the experiment, peaking at 6.68 mg(N)/L after 17 days at 72 cm depth and at 3.13 mg(N)/L after 66 days at 27 cm depth (Fig. 1). Concentrations were above the EU Water Framework Directive limit for the first ~100 days in samples from 27 cm depth and the first ~360 days in samples from 72 cm depth. Ammonium concentrations plotted against cumulative flow volume, used for trapezoidal integration to calculate the mass, are shown in Figure S3. The resulting ammonium nitrogen masses of 0.41 g passing 27 cm depth and 1.2 g passing 72 cm depth are shown on Fig. 1. The end-of-wetting sampling of CI shows that if TWW were infiltrated through this soil in a field MAR scheme, it would send a plume of ammonium to the aquifer.

3.1.2. Drying periods

Samples collected using the first flush technique contain a mixture of inflow water and pore water, in its condition at the end of the drying period. To observe the proportion of inflow water in the collected samples, sodium bromide was added to the inflow water for first flush sampling conducted at the end of the 13th drying period (bromide C_0 = 11.5 mg/L, with background concentrations from the end of the previous wetting period < 0.5 mg/L). Analyzed concentrations of the

soil pore water samples compared to the inflow water showed bromide C/C_0 of 0.49 (2 cm depth), 0.45 (7 cm), 0.23 (27 cm), 0.18 (57 cm), and 0.29 (72 cm). Based on these results, it is presumed that all first flush samples contain some pore water, likely a portion $\geq \sim 0.7$ at 27 cm and greater depths. This pore water is thought to have been mobilized along the infiltration flow path to the sampling port.

Concentrations of nitrate in first flush and end of wetting samples from a selected portion of the experiment are shown in Fig. 2. Concentrations of nitrate rose substantially during the drying periods, as the pore water-inflow water mixture contained higher concentrations of nitrate than the inflow water in most cases, except for 72 cm depth. The highest concentrations of nitrate were found in samples from 27 cm depth. Although the pore water in the sample could have originated anywhere from the soil surface down to the sampling port, at 27 cm depth, elevated concentrations of ammonium during the wetting periods coincide with replenishment of oxygen during the drying periods (Fig. 3), providing both mass of ammonium and potential for nitrification. At 72 cm depth, oxygen concentrations were near or below detection limits and nitrate concentrations in the first flush samples were 0.15 mg(N)/L or lower (except for Day 136, 1.1 mg(N)/L). Based on the higher nitrate concentrations at depths other than 72 cm, it appears likely that nitrification of ammonium occurred during the drying periods, as was reported by Miller et al. (2006) and Hernández-Martínez et al. (2016).

At depths between 12 and 42 cm, oxygen concentrations at the end of the wetting periods increased slightly through time (Fig. 3). This may indicate depletion of labile organic carbon from the soil and/or residual TWW, such that less anaerobic respiration occurred in successively later drying periods. Below about 50 cm, the soil remained water saturated during the drying periods, resulting in near-zero oxygen concentrations. Decreases in concentration of ammonium in the first flush samples (Figure S4), compared to the previous wetting period, were observed fairly consistently at 57 cm depth, but they do not correspond in magnitude to the increases in nitrate concentration. At 72 cm depth, first flush ammonium concentrations were higher than during the wetting periods. However, the column remained close to saturation here during the drying periods, so possibly ammonium may have continued to form with stagnant water present in the pore space. At other depths, first flush concentrations were similar to those measured in samples from the end of wetting periods. The lack of a clear trend toward lower ammonium concentrations in first flush samples could be due to variation in the inflow water ammonium concentration and/or possible desorption of ammonium as concentrations lowered, preventing large fluctuations in concentration.

3.2. Short-term experiment

The long-term experiment showed that ammonium concentrations rise during infiltration of treated wastewater through the experimental soil and that some ammonium may be nitrified during drying periods. In the short-term experiment, nitrogen cycling was investigated in more detail by collecting stable isotope, ORP and acetate data.

3.2.1. Oxidation reduction potential

ORP measurements illustrate a clear difference in redox conditions between the wetting and drying periods (Fig. 4). During wetting phases, Eh reached approximately -200 mV at all depths. This Eh is similar to that found by Dhondt et al. (2003) during autumn and winter, a time period for which they show that DNRA was responsible for at least some nitrate reduction. In the present study, reducing conditions were present everywhere in the soil during wetting periods. During drying phases, Eh recovered to ~400 mV in the upper part of the soil, while remaining essentially unchanged from 45 cm downward. The soil remained water saturated during the drying periods from ~50 cm depth downward. Beginning on Day 104, a tracer test was conducted, with a wetting length of 15 days, resulting in an extended time period with Eh

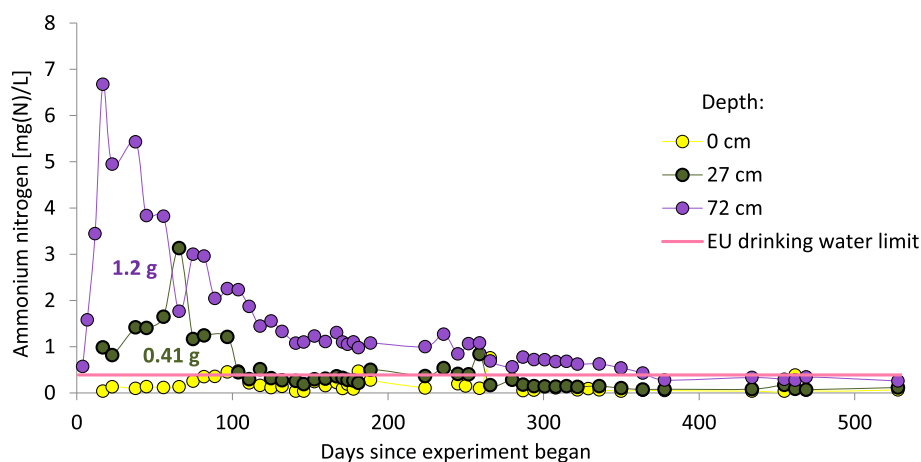


Fig. 1. Ammonium nitrogen concentrations measured during the long-term experiment relative to the EU drinking water limit.

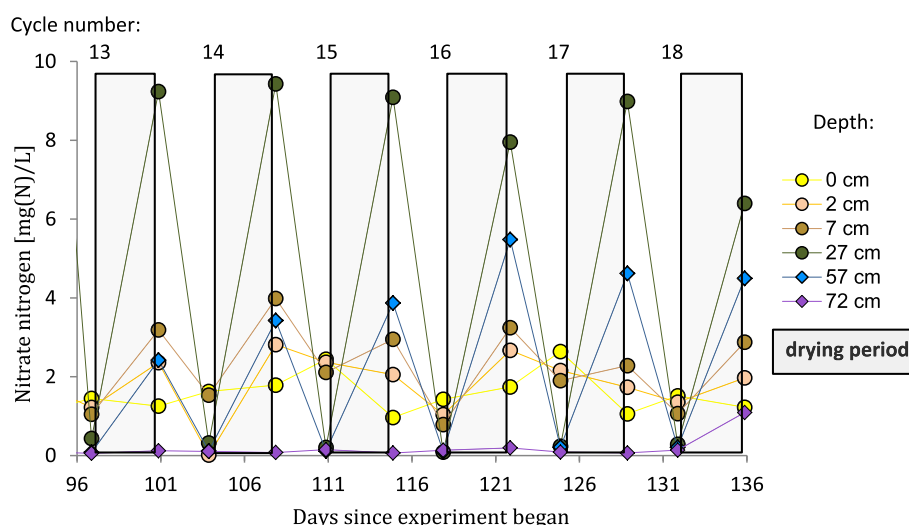


Fig. 2. Nitrate nitrogen concentrations measured during end of wetting and first flush sampling during a selected portion of the long-term experiment. First flush samples (immediately following the end of each drying period) contain a mixture of drying period pore water and inflow water.

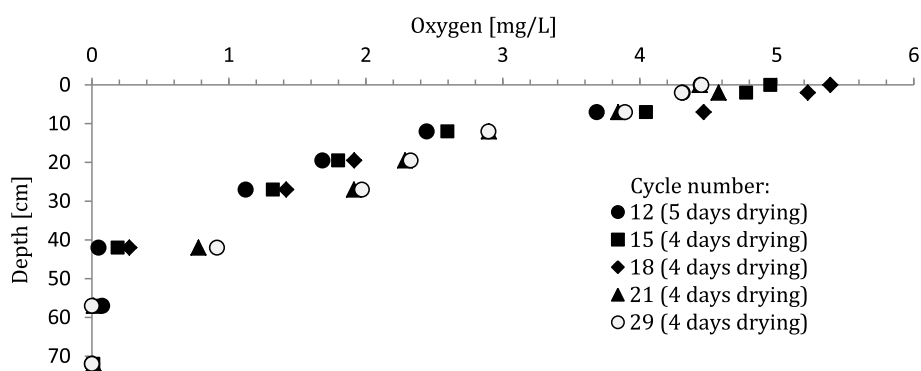


Fig. 3. Oxygen concentrations decreased with depth in the soil at the end of drying periods in the long-term experiment.

around -200 mV at all depths.

The maximum Eh reached during drying periods at 15 cm depth was low through the 11th drying (\sim Day 75) and then was substantially higher during the following drying periods. A similar trend was observed in oxygen concentrations, which are shown in Figure S5. The increase in oxygen concentration and Eh in later wetting periods may have resulted from depletion of the system of labile organic carbon (e.g. acetate), so that less anaerobic respiration occurred.

With the oxidizing conditions in the upper part of the soil, the

potential for nitrification of ammonium was present. The interpretation that ammonium is nitrified during drying periods is also consistent with the higher nitrate concentrations found during first flush sampling (section 3.1.2). In studies infiltrating TWW in which ammonium was the dominant form of inorganic nitrogen, some ammonium is nitrified during drying periods and then denitrified during wetting periods, with retention of ammonium in the soil appearing to play a role (Miller et al., 2006; Hernández-Martínez et al., 2016).

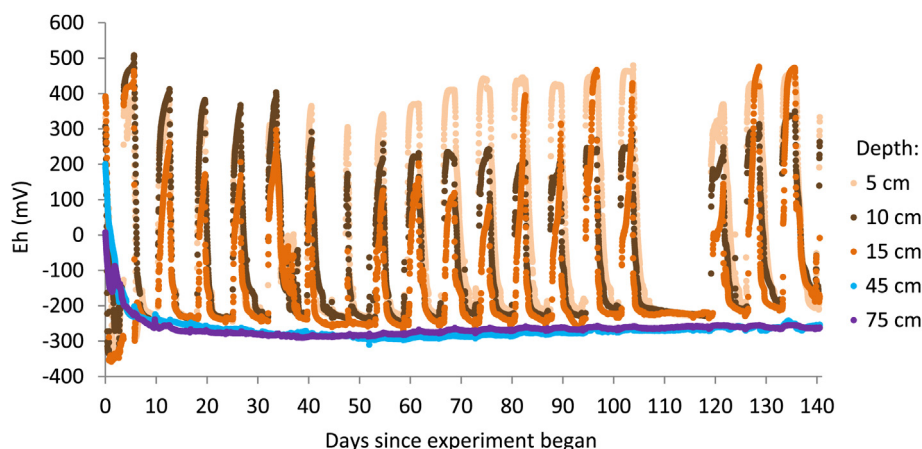


Fig. 4. Eh measurements show a wide range of redox conditions during wetting and drying cycles in the shallow soil, while Eh remained constant at greater depth.

3.2.2. Acetate

Acetate is a form of labile organic carbon. It can be formed in soils by anaerobic decomposition of a variety of plant substances (Acharya, 1935), which our experimental soil contained in the form of fragments of roots and plant stems. While acetate is commonly produced through fermentation of more complex forms of organic matter, it can then act as an electron donor in denitrification (Paul and Beauchamp, 1989) or DNRA (van den Berg et al., 2017). Acetate concentrations were highest in the beginning of the experiment and at depth in the soil (Fig. 5).

In considering possible sources of the ammonium, it has been shown that with higher labile organic carbon to nitrate ratios, nitrate reduction is driven from denitrification toward DNRA (Buresh and Patrick, 1978; Yin et al., 2002; Yoon et al., 2015). Jørgensen (1989) found that denitrification occurred close to the soil surface but that nitrate reduction switched to DNRA with increasing depth, in as little as 1 cm from the soil surface. Based on the occurrence of high acetate concentrations, the conditions needed for DNRA may have been present in the earlier stages of the experiment and at greater depths in the soil. van den Berg et al. (2016) showed that at acetate to nitrate molar ratios of ~ 1 and higher, DNRA occurred (to some extent concurrently with denitrification) in activated sludge taken from a wastewater treatment plant. In our short-term experiment, acetate and nitrate were both above detection limits in many samples from 15 cm to 30 cm depth, particularly early in the experiment. In these samples, the acetate to nitrate molar ratio was always 8 or higher, indicating the presence of conditions under which DNRA occurs.

A local peak in acetate concentrations is seen in the fourth sampling event, which was performed at the end of a wetting phase in which the flow rate was lowered due to technical problems with column operation. The slower water flow results in longer contact time for the water with the soil, which might have allowed higher production of acetate.

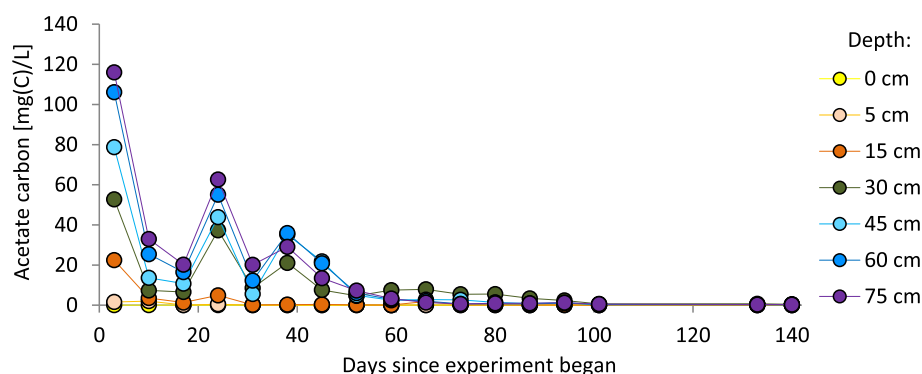


Fig. 5. Acetate carbon concentrations in inflow and pore water over the course of the short-term experiment.

3.2.3. Ammonium

Ammonium concentrations in the short-term experiment rose to as high as 13.94 mg(N)/L (Fig. 6). The pattern over time was similar to CI, with concentrations peaking after 38 days at 30 cm depth and 52 days at 75 cm depth, although a less pronounced second peak is seen at some depths. Ammonium was present in the beginning at all measured depths, but then generally decreased progressively over time with depth. Results from the fourth sampling event (24 days) were slightly higher than in the fifth sampling event, showing a local peak. The local peak in ammonium concentrations seen in the fourth sampling (24 days) may be due to the flow conditions described in section 3.2.2. Ammonium concentrations plotted against cumulative flow volume are shown in Figure S6.

The short-term experiment (CII) lasted for 140.5 days, during which a total of 113 L of TWW was infiltrated. Based on the flow volume at sampling times and ammonium nitrogen concentrations shown in Figure S6, 0.78 g(N) of ammonium was observed in the water at 75 cm depth. In CII, 0.26 g(N) of nitrate was infiltrated. Compared to the 0.78 g(N) of ammonium at 75 cm depth, not enough nitrate was infiltrated to account for all of the mass of ammonium observed. If inflow DON remained in the range of 1.4–2.1 mg/L (high and low values measured, discussed further in the SI) over the duration of the experiment, the mass of DON infiltrated was in the range of 0.16–0.24 g(N), which is also not enough to account for all of the ammonium formed. Further, when the infiltrated masses of nitrate and assumed DON are summed, 0.38–0.50 g(N) was infiltrated, compared to 0.78 g(N) of ammonium observed at 75 cm depth. As the mass of infiltrated nitrogen appears to be less than the mass of ammonium, it is likely that soil nitrogen was a source for at least some of the ammonium. Approximately 55 g of nitrogen was present in the soil between the surface and 75 cm depth (see SI).

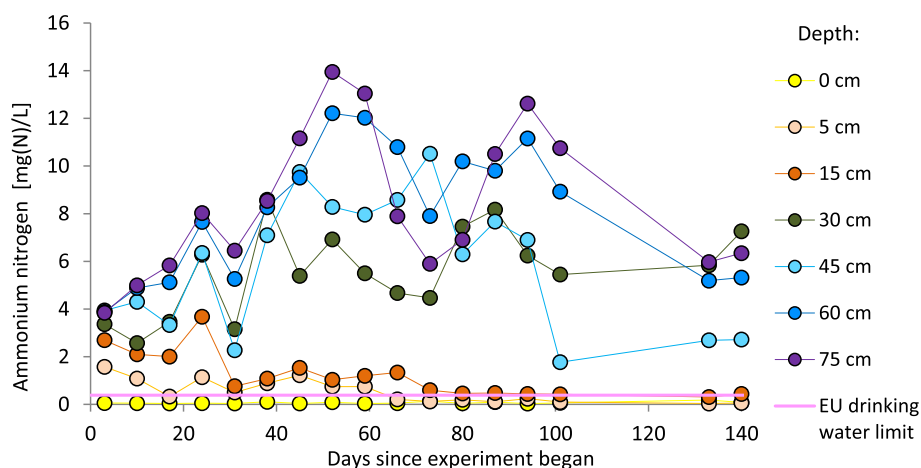


Fig. 6. Ammonium nitrogen concentrations in pore water samples over the course of the short-term experiment.

In CI, with the higher flow rate, only 0.33 g(N) of ammonium was observed at 72 cm depth through a flow volume of 110 L (37.7 days), the total flow volume through CII. However, comparing equal time intervals, 0.83 g(N) of ammonium was observed through 140.7 days in CI (311 L of cumulative flow, almost three times the flow volume through CII for the same amount of time), which is close to the 0.78 g(N) of ammonium at 75 cm depth in CII (140.5 days). Thus, it appears that longer reaction time allows for more ammonium formation and that time, rather than flow volume, appears to have been the more critical factor in how much mass of ammonium formed. Thus, in addition to the mass balance, the similarity of the temporal pattern suggests that the soil was a prominent source of the ammonium because if the main source of the ammonium were in the TWW, flow rate should have had an influence on how much ammonium forms.

3.2.4. Stable isotopes in nitrate

Results of $\delta^{15}\text{N-NO}_3$ and $\delta^{18}\text{O-NO}_3$ for all samples from 0 to 15 cm depth are shown in Fig. 7. Samples from 5 cm depth are overall more enriched in ^{15}N and ^{18}O than the inflow (0 cm depth), and samples from 15 cm depth are overall more enriched in the heavy isotopes than the samples from 5 cm depth. Results for individual sampling events are shown in Figure S7 and consistently show enrichment of ^{15}N and ^{18}O at 5 cm depth relative to the 0 cm sample for the respective wetting period (with the exception of ^{15}N in the 13th wetting period). Where isotopes were detected in samples from 15 cm depth, in most cases these also show enrichment relative to the 5 cm sample from the same wetting period. Overall, these observations are consistent with studies using dual isotopes that clearly show the occurrence of denitrification (e.g.,

Böttcher et al., 1990; Mengis et al., 1999). Further, the $\delta^{15}\text{N}$ versus natural log-normalized nitrate concentration was in many cases linear between 0 cm and 15 cm depth (5 wetting periods out of 9 with isotope detection at all three depths; Figure S7). Such a linear relationship can result from denitrification (Mariotti et al., 1981). In some other cases (see SI) the slope becomes shallower with either the 15 cm or 30 cm sample; this could be a result of nitrate reduction switching (partially) to DNRA. While in general enrichment of ^{15}N and ^{18}O is apparent in the data, when all of the data points are viewed together as in Fig. 7, considerable variation from the linear relationship that is expected for denitrification is seen. This variation is likely a result of signal interference from multiple processes, some of which may have occurred concurrently in different micro-environments within the porous medium.

One process that could interfere with the signal is DNRA. Rayleigh enrichment factors based on the concentration- ^{15}N relationship resulting from denitrification typically range from about -11 to -33% , with lower absolute values likely being associated with faster reaction rates (Mariotti et al., 1982). Overall in our study, the mean apparent enrichment factor based on the 0 and 5 cm samples and Equation (1) was -7.2% but with considerable variation between wetting periods (Figure S7). These values overall do not seem to be consistent with denitrification as a single enrichment process. Dhondt et al. (2003) found a nitrate ^{15}N enrichment factor of -6.2% that likely was influenced by DNRA as a competing process with denitrification. In our system, it may also be that denitrification and DNRA were competing nitrate reduction processes, with variation in apparent enrichment factors due to relative predominance of one process over the other.

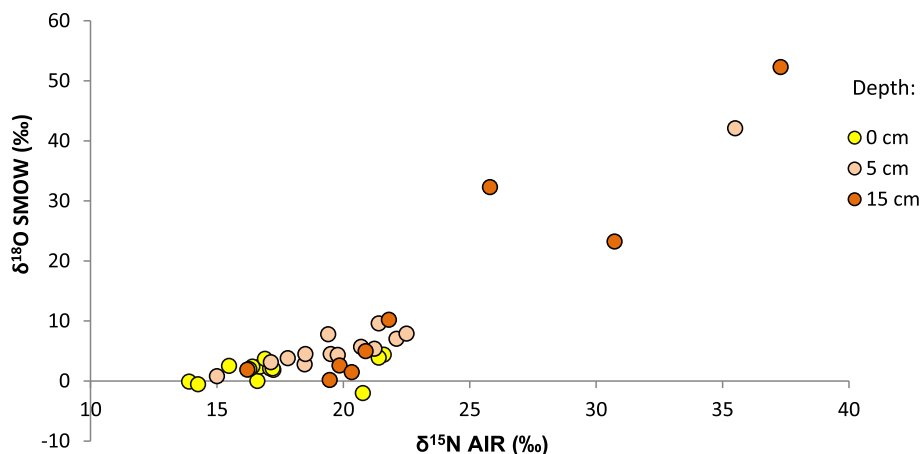


Fig. 7. Dual isotope plot of ^{15}N and ^{18}O in all samples analyzed over the course of the experiment.

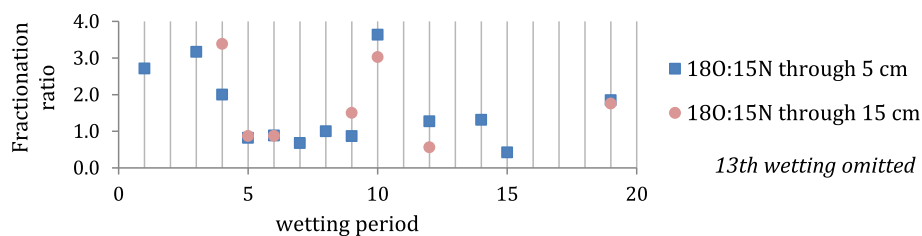


Fig. 8. $^{18}\text{O}:^{15}\text{N}$ fractionation ratios over the course of the experiment.

Chen and Macquarrie (2005) evaluated nitrate dual isotope data in six studies in which denitrification likely occurred, finding $^{18}\text{O}:^{15}\text{N}$ fractionation ratios in the range of 0.48–0.67, while Carrey et al. (2014) found a ratio of 0.93. In our study, the slope of dual isotope plots for individual wetting periods (Fig. 8) is outside of this range for a substantial number of wetting periods. Higher enrichment of O relative to N is seen in the earlier wetting periods, when the higher acetate concentrations were present, a factor which is thought to drive nitrate reduction toward DNRA. In a column study with lake sediments, DNRA was inferred to have occurred in the early stages of infiltration (Carrey et al., 2014).

In some samples from 30 cm and deeper, nitrate concentration was sufficient to detect isotopic ratios. In these cases, $\delta^{15}\text{N}\text{-NO}_3$ became lighter with depth (Figure S7) and in some cases lighter than the inflow (2nd, 4th and 19th wetting phases). This indicates the presence of an additional, isotopically lighter nitrogen source in the soil pore water contributing to the nitrate pool. A lighter nitrogen source that was present is ammonium (results follow in section 3.2.5 and Fig. 9). The isotopically lighter nitrate-nitrogen provides evidence, in addition to the first flush sampling results (section 3.1.2), that nitrification of ammonium occurred during the drying periods. The fact that this lighter nitrate-nitrogen is only (with the exception of the 13th wetting) found at greater depths (30 cm and deeper) is consistent with the interpretation that it formed during the previous drying period and then was flushed downward during the next wetting period, at the end of which sampling was conducted.

3.2.5. Stable isotopes of ammonium and its possible sources

Stable isotopes of ammonium and its possible sources are shown in Fig. 9. $\delta^{15}\text{N}\text{-NH}_4^+$ is similar to $\delta^{15}\text{N}\text{-Soil}$, although in most samples the ammonium is isotopically somewhat heavier than the soil nitrogen. Because of the similarity, the soil nitrogen is a likely source of at least some of the ammonium. Most of the $\delta^{15}\text{N}\text{-NH}_4^+$ values are higher than

the $\delta^{15}\text{N}\text{-soil}$ value, which is likely an effect of nitrification during the drying periods and/or DNRA during the wetting periods. Nitrification would result in isotopically lighter nitrate-nitrogen, leaving isotopically heavier ammonium-nitrogen behind in the portion of ammonium that remained at the end of the drying periods. DNRA would convert nitrogen from the isotopically heavier nitrate (Fig. 9) to ammonium. With the soil as a main source of the ammonium, it is likely that the $\delta^{15}\text{N}\text{-NH}_4^+$ values are increased from the value of the $\delta^{15}\text{N}\text{-soil}$ through a combination of both DNRA (wetting periods) and nitrification (drying periods). While nitrate is a possible source for some of the ammonium, DON in the inflow water appears to be isotopically similar to or lighter than the soil. Thus, DON does not appear to be an important source of the ammonium.

At 30 cm depth, $\delta^{15}\text{N}\text{-NH}_4^+$ rose in the beginning to a maximum of 10.3‰ on Day 17, then declined thereafter. As ammonium may be retarded in the soil, the peak on Day 17 may be an additional indication that ammonium formed from an isotopically heavier source (nitrate) in the early stages of infiltration, with this source becoming less important over time. The high concentrations of acetate in the early stages of the experiment (Fig. 5) provided a labile carbon source that has been shown to drive the nitrate reduction system toward DNRA (van den Berg et al., 2016).

4. Conclusions

In two separate column experiments infiltrating TWW through a natural soil, ammonium was produced during infiltration. Based on mass balance and isotopic data, soil nitrogen appears to be an important source of the ammonium, if not the main source. While soils with high organic matter content have certain advantages for MAR, implementers of MAR schemes should be aware of the potential to form ammonium with concentrations exceeding the EU water framework directive limit in the infiltrating water. As ammonium concentrations

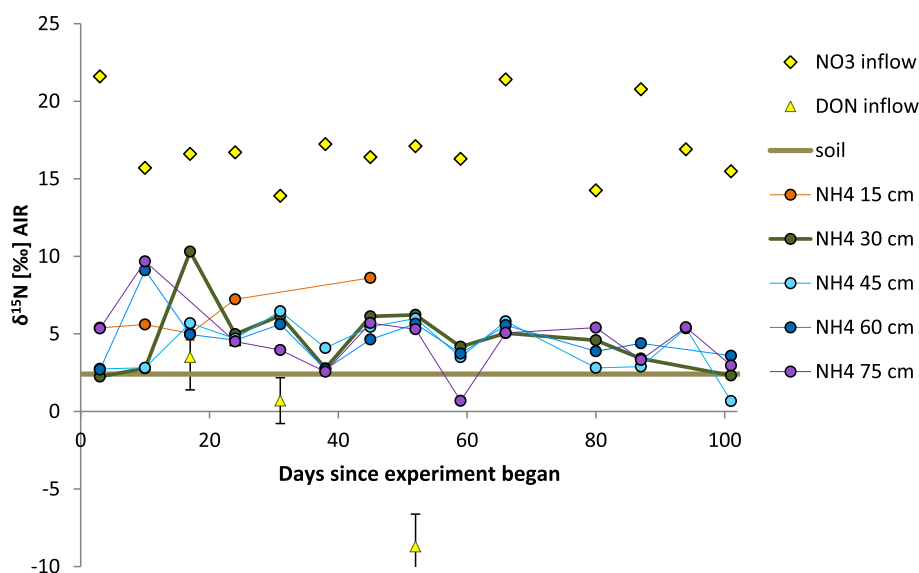


Fig. 9. $\delta^{15}\text{N}$ in ammonium in comparison to $\delta^{15}\text{N}$ in the soil nitrogen, inflow water nitrate, and inflow water DON.

first increased to an initial peak and then decreased, MAR applications should be planned with the view that ammonium might be generated during an initial phase of infiltration.

Our results suggest that nitrification occurs during drying phases and a combination of denitrification and DNRA during wetting phases. While denitrification of at least some of the nitrate in the inflow TWW appears to have occurred, several indications of DNRA were also observed: high acetate:nitrate ratios early in the experiments and in the 15–30 cm depth range in the soil, Eh values below zero and often below –200 during wetting periods, high $\delta^{15}\text{N}$ of nitrate in the inflow water combined with $\delta^{15}\text{N}$ of ammonium greater than that of the soil and that increased early in the experiment, and isotopic enrichment factors that are lower than enrichment factors typically found for denitrification occurring alone. The high $^{18}\text{O}:^{15}\text{N}$ ratios may also be a result of DNRA, although this warrants further research. For implementation of MAR schemes, the occurrence of DNRA is important in that it lowers the nitrogen elimination rate of the system. As opposed to gaseous products of denitrification, nitrate-nitrogen reduced to ammonium will remain in the system, either as ammonium or later nitrified back to nitrate. This cycling of ionic nitrogen forms presents the potential to deliver a plume of ammonium and/or nitrate to the aquifer.

As ammonium is retarded during transport through many soils and aquifer materials, if drying phases can effectively introduce oxygen into the subsurface, our experiments suggest that some ionic nitrogen mass may be eliminated by nitrification during drying periods and denitrification during the subsequent wetting period. Further research could focus on the partitioning of nitrate reduction between denitrification (eliminating nitrogen mass from the system) and DNRA (conservation of nitrogen mass in the system). The length of wetting and drying cycles, particularly in the beginning of infiltration when concentrations of acetate and other labile organic carbon compounds are likely to be high, may be a tool to influence partitioning between denitrification and DNRA and thereby how much nitrogen mass is conserved in the MAR system.

Declarations of interest

None.

Acknowledgements

The research leading to these results received funding from the European Union Seventh Framework Programme (FP7/2007–2013) under grant agreement no. 619120 (Demonstrating Managed Aquifer Recharge as a Solution to Water Scarcity and Drought – MARSOL). Additionally, the authors thank Rainer Kurdum and Patrick Marschall for assistance with sample collection and column construction in the course of their master's theses.

Appendix A. Supplementary data

Supplementary data related to this article can be found at <https://doi.org/10.1016/j.apgeochem.2018.08.003>.

References

- Acharya, C.N., 1935. Studies on the anaerobic decomposition of plant materials. IV. The decomposition of plant substances of varying composition. *Biochem. J.* 29, 1459–1467.
- Barry, K.E., Vanderzalm, J.L., Miotlinski, K., Dillon, P.J., 2017. Assessing the impact of recycled water quality and clogging on infiltration rates at a pioneering Soil Aquifer Treatment (SAT) site in Alice Springs, Northern Territory (NT), Australia. *Water (Switzerland)* 9. <https://doi.org/10.3390/w9030179>.
- Bekele, E., Toze, S., Patterson, B., Higginson, S., 2011. Managed aquifer recharge of treated wastewater: water quality changes resulting from infiltration through the vadose zone. *Water Res.* 45, 5764–5772. <https://doi.org/10.1016/j.watres.2011.08.058>.
- Böttcher, J., Strebel, O., Voerkelius, S., Schmidt, H.L., 1990. Using isotope fractionation of nitrate-nitrogen and nitrate-oxygen for evaluation of microbial denitrification in a sandy aquifer. *J. Hydrol.* 114, 413–424. [https://doi.org/10.1016/0022-1694\(90\)90068-9](https://doi.org/10.1016/0022-1694(90)90068-9).
- Bouwer, H., 2002. Artificial recharge of groundwater: hydrogeology and engineering. *Hydrogeol. J.* 10, 121–142. <https://doi.org/10.1007/s10040-001-0182-4>.
- Buresh, R.J., Patrick, W.H.J., 1978. Nitrate reduction to ammonium in anaerobic soil. *Soil Sci. Soc. Am. J.* 42, 913–918.
- Carrey, R., Rodríguez-Escobedo, P., Otero, N., Ayora, C., Soler, A., Gómez-Alday, J.J., 2014. Nitrate attenuation potential of hypersaline lake sediments in central Spain: flow-through and batch experiments. *J. Contam. Hydrol.* 164, 323–337. <https://doi.org/10.1016/j.jconhyd.2014.06.017>.
- Caschetto, M., Colombani, N., Mastrocicco, M., Petitta, M., Aravena, R., 2017. Nitrogen and sulphur cycling in the saline coastal aquifer of Ferrara, Italy. A multi-isotope approach. *Appl. Geochem.* 76, 88–98. <https://doi.org/10.1016/j.apgeochem.2016.11.014>.
- Casciotti, K.L., Sigman, D.M., Hastings, M.G., Böhlke, J.K., Hilkert, A., 2002. Measurement of the oxygen isotopic composition of nitrate in seawater and freshwater using the denitrifier method. *Anal. Chem.* 74, 4905–4912. <https://doi.org/10.1021/ac020113w>.
- Chen, D.J.Z., Macquarrie, K.T.B., 2005. Correlation of $\delta^{15}\text{N}$ and $\delta^{18}\text{O}$ in NO_3^- during denitrification in groundwater. *J. Environ. Eng. Sci.* 226, 221–226. <https://doi.org/10.1139/S05-002>.
- Czerwionka, K., Makinia, J., Pagilla, K.R., Stensel, H.D., 2012. Characteristics and fate of organic nitrogen in municipal biological nutrient removal wastewater treatment plants. *Water Res.* 46, 2057–2066. <https://doi.org/10.1016/j.watres.2012.01.020>.
- Dhondt, K., Boeckx, P., Van Cleemput, O., Hofman, G., 2003. Quantifying nitrate retention processes in a riparian buffer zone using the natural abundance of ^{15}N in NO_3^- . *Rapid Commun. Mass Spectrom.* 17, 2597–2604. <https://doi.org/10.1002/rcm.1226>.
- Dutta, T., Carles-Brangarí, A., Fernández-García, D., Rubol, S., Tirado-Conde, J., Sanchez-Vila, X., 2015. Vadose zone oxygen (O_2) dynamics during drying and wetting cycles: an artificial recharge laboratory experiment. *J. Hydrol.* 527, 151–159. <https://doi.org/10.1016/j.jhydrol.2015.04.048>.
- Essandoh, H.M.K., Tizaoui, C., Mohamed, M.H.A., Amy, G., Brdjanovic, D., 2011. Soil aquifer treatment of artificial wastewater under saturated conditions. *Water Res.* 45, 4211–4226. <https://doi.org/10.1016/j.watres.2011.05.017>.
- Goren, O., Burg, A., Gavrieli, I., Negev, I., Guttman, J., Kraitzer, T., Kloppmann, W., Lazar, B., 2014. Biogeochemical processes in infiltration basins and their impact on the recharging effluent, the soil aquifer treatment (SAT) system of the Shafdan plant. *Israel. Appl. Geochemistry* 48, 58–69. <https://doi.org/10.1016/j.apgeochem.2014.06.017>.
- Hadas, A., Sofer, M., Molina, J.A.E., Barak, P., Clapp, C.E., 1992. Assimilation of nitrogen by soil microbial population: NH_4 versus organic N. *Soil Biol. Biochem.* 24, 137–143. [https://doi.org/10.1016/0038-0717\(92\)90269-4](https://doi.org/10.1016/0038-0717(92)90269-4).
- Hernández-Martínez, J.L., Prado, B., Cayetano-Salazar, M., Bischoff, W.A., Siebe, C., 2016. Ammonium-nitrate dynamics in the critical zone during single irrigation events with untreated sewage effluents. *J. Soils Sediments* 1–14. <https://doi.org/10.1007/s11368-016-1506-2>.
- Jørgensen, K.S., 1989. Annual pattern of denitrification and nitrate ammonification in estuarine sediment. *Appl. Environ. Microbiol.* 55, 1841–1847.
- Kopchynski, T., Fox, P., Alsmadi, B., Berner, M., 1996. The effects of soil type and effluent pre-treatment on soil aquifer treatment. *Water Sci. Technol.* 34, 235–242. [https://doi.org/10.1016/S0273-1223\(96\)00843-8](https://doi.org/10.1016/S0273-1223(96)00843-8).
- Kraft, B., Tegetmeyer, H.E., Sharma, R., Klotz, M.G., Ferdelman, T.G., Hettich, R.L., Geelhoed, J.S., Strous, M., 2014. The environmental controls that govern the end product of bacterial nitrate respiration. *Science* 345 (80), 676–679. <https://doi.org/10.1126/science.1254070>.
- Krata, A., Kontozova-Deutsch, V., Bencs, L., Deutsch, F., Van Grieken, R., 2009. Single-run ion chromatographic separation of inorganic and low-molecular-mass organic anions under isocratic elution: application to environmental samples. *Talanta* 79, 16–21. <https://doi.org/10.1016/j.talanta.2009.02.044>.
- Lingle, D.A., Kehew, A.E., Krishnamurthy, R.V., 2017. Use of nitrogen isotopes and other geochemical tools to evaluate the source of ammonium in a confined glacial drift aquifer, Ottawa County, Michigan, USA. *Appl. Geochem.* 78, 334–342. <https://doi.org/10.1016/j.apgeochem.2017.01.004>.
- Maeng, S.K., Sharma, S.K., Lekkerkerker-Teunissen, K., Amy, G.L., 2011. Occurrence and fate of bulk organic matter and pharmaceutically active compounds in managed aquifer recharge: a review. *Water Res.* 45, 3015–3033. <https://doi.org/10.1016/j.watres.2011.02.017>.
- Mania, D., Heylen, K., van Spanning, R.J., Frostegård, A., 2014. The nitrate-ammonifying and nosZ-carrying bacterium *Bacillus vireti* is a potent source and sink for nitric and nitrous oxide under high nitrate conditions. *Environ. Microbiol.* 16, 3196–3210. <https://doi.org/10.1111/1462-2920.12478>.
- Mariotti, A., Germon, J.C., Hubert, P., Kaiser, P., Letolle, R., Tardieux, A., Tardieux, P., 1981. Experimental determination of nitrogen kinetic isotope fractionation: some principles; illustration for the denitrification and nitrification processes. *Plant Soil* 62, 413–430. <https://doi.org/10.1007/BF02374138>.
- Mariotti, A., Germon, J.C., Leclerc, A., 1982. Nitrogen isotope fractionation associated with the $\text{NO}_2^- \rightarrow \text{N}_2\text{O}$ step of denitrification in soils. *Can. J. Soil Sci.* 62, 227–241.
- McIlvin, M.R., Casciotti, K.L., 2011. Technical updates to the bacterial method for nitrate isotopic analyses. *Anal. Chem.* 83, 1850–1856. <https://doi.org/10.1021/ac1028984>.
- Mengis, M., Schiff, S.L., Harris, M., English, M.C., Aravena, R., Elgood, R.J., MacLean, A., 1999. Multiple geochemical and isotopic approaches for assessing ground water NO_3^- Elimination in a riparian zone. *Ground Water*. <https://doi.org/10.1111/j.1745-6584.1999.tb01124.x>.
- Miller, J.H., Ela, W.P., Lansey, K.E., Chipello, P.L., Arnold, R.G., 2006. Nitrogen transformations during soil-aquifer treatment of wastewater effluent—oxygen effects in

- field studies. *J. Environ. Eng.* 132, 1298–1306. [https://doi.org/10.1061/\(ASCE\)0733-9372\(2006\)132:10\(1298\)](https://doi.org/10.1061/(ASCE)0733-9372(2006)132:10(1298)).
- Miotłinski, K., Barry, K., Dillon, P., Breton, M., 2010. Alice Springs SAT Project Hydrological and Water Quality Monitoring. Report 2008–2009.
- Morugán-Coronado, A., García-Orenes, F., Mataix-Solera, J., Arcenegui, V., Mataix-Beneyto, J., 2011. Short-term effects of treated wastewater irrigation on Mediterranean calcareous soil. *Soil Tillage Res.* 112, 18–26. <https://doi.org/10.1016/j.still.2010.11.004>.
- Murphy, D.V., Recous, S., Stockdale, E.A., Fillery, I.R.P., Jensen, L.S., Hatch, D.J., Goulding, K.W.T., 2003. Gross nitrogen fluxes in soil: theory, measurement and application of 15N pool dilution techniques. *Adv. Agron.* 79, 69–118. [https://doi.org/10.1016/S0065-2113\(02\)79002-0](https://doi.org/10.1016/S0065-2113(02)79002-0).
- Parkin, G.F., McCarty, P.L., 1981. A comparison of the characteristics of soluble organic nitrogen in untreated and activated sludge treated wastewaters. *Water Res.* 15, 139–149. [https://doi.org/10.1016/0043-1354\(81\)90194-9](https://doi.org/10.1016/0043-1354(81)90194-9).
- Patton, C.J., Kryskalla, J.R., 2003. Methods of Analysis by the U.S. Geological Survey National Water Quality Laboratory: Evaluation of Alkaline Persulfate Digestion as an Alternative to kjeldahl Digestion for Determination of Total and Dissolved Nitrogen and Phosphorus in Water. Water-Resources Investigations Report 03-4174. .
- Paul, J.W., Beauchamp, E.G., 1989. Denitrification and fermentation in plant-residue-amended soil. *Biol. Fertil. Soils* 7, 303–309. <https://doi.org/10.1007/BF00257824>.
- Powelson, D.K., Gerba, C.P., Yahya, M.T., 1993. Virus transport and removal in wastewater during aquifer recharge. *Water Res.* 27, 583–590. [https://doi.org/10.1016/0043-1354\(93\)90167-G](https://doi.org/10.1016/0043-1354(93)90167-G).
- Schmidt, C.M., Fisher, A.T., Racz, A., Wheat, C.G., Los Huertos, M., Lockwood, B., 2012. Rapid nutrient load reduction during infiltration of managed aquifer recharge in an agricultural groundwater basin: pajaro Valley, California. *Hydrol. Process.* 26, 2235–2247. <https://doi.org/10.1002/hyp.8320>.
- Sigman, D.M., Casciotti, K.L., Andreani, M., Barford, C., Galanter, M., Böhlke, J.K., 2001. A bacterial method for the nitrogen isotopic analysis of nitrate in seawater and freshwater. *Anal. Chem.* 73, 4145–4153. <https://doi.org/10.1021/ac010088e>.
- Silver, M., Selke, S., Balsaa, P., Wefer-roehl, A., Kübeck, C., Schüth, C., 2018. Fate of five pharmaceuticals under different infiltration conditions for managed aquifer recharge. *Sci. Total Environ.* 642, 914–924. <https://doi.org/10.1016/j.scitotenv.2018.06.120>.
- Stanford, G., Smith, S.J., 1972. Nitrogen mineralization potentials of soils. *Soil Sci. Soc. Am. J.* 36, 465–472. <https://doi.org/10.2136/sssaj1972.03615995003600030029x>.
- The Council of the European Union, 2000. Directive 2000/60/EC of the European Parliament and of the Council of 23 October 2000 establishing a framework for Community action in the field of water policy. Official Journal of the European Parliament. <https://doi.org/10.1039/ap9842100196>.
- The Council of the European Union, 1998. Council Directive 98/83/EC of 3 November 1998 on the quality of water intended for human consumption. Official Journal of the European Communities doi:2004R0726-v.7.of.05.06.2013.
- Valhondo, C., Carrera, J., Ayora, C., Tubau, I., Martínez-Landa, L., Nödler, K., Licha, T., 2015. Characterizing redox conditions and monitoring attenuation of selected pharmaceuticals during artificial recharge through a reactive layer. *Sci. Total Environ.* 512–513, 240–250. <https://doi.org/10.1016/j.scitotenv.2015.01.030>.
- van den Berg, E.M., Boleij, M., Kuenen, J.G., Kleerebezem, R., van Loosdrecht, M.C.M., 2016. DNRA and denitrification coexist over a broad range of acetate/N-NO₃⁻ ratios, in a chemostat enrichment culture. *Front. Microbiol.* 7, 1–12. <https://doi.org/10.3389/fmicb.2016.01842>.
- van den Berg, E.M., Elisário, M.P., Kuenen, J.G., Kleerebezem, R., van Loosdrecht, M.C.M., 2017. Fermentative bacteria influence the competition between denitrifiers and DNRA bacteria. *Front. Microbiol.* 8, 1–13. <https://doi.org/10.3389/fmicb.2017.01684>.
- Vorenhout, M., van der Geest, H.G., van Marum, D., Wattel, K., Eijsackers, H.J.P., 2004. Automated and continuous redox potential measurements in soil. *J. Environ. Qual.* 33, 1562–1567. <https://doi.org/10.2134/jeq2004.1562>.
- Yin, S.X., Chen, D., Chen, L.M., Edis, R., 2002. Dissimilatory nitrate reduction to ammonium and responsible microorganisms in two Chinese and Australian paddy soils. *Soil Biol. Biochem.* 34, 1131–1137. [https://doi.org/10.1016/S0038-0717\(02\)00049-4](https://doi.org/10.1016/S0038-0717(02)00049-4).
- Yoon, S., Cruz-García, C., Sanford, R., Ritalahti, K.M., Löffler, F.E., 2015. Denitrification versus respiratory ammonification: environmental controls of two competing dissimilatory NO₃⁻/NO₂⁻ reduction pathways in *Shewanella loihica* strain PV-4. *ISME J.* 9, 1093–1104. <https://doi.org/10.1038/ismej.2014.201>.